Prompt Photon Production at the Tevatron*

STEFAN SÖLDNER-REMBOLD

University of Manchester
School of Physics and Astronomy
Manchester M13 9PL
United Kingdom

on behalf of the DØ and CDF Collaborations

The DØ and CDF experiments have measured prompt photon production using Run II data taken at a centre-of-mass energy $\sqrt{s}$ of 1.96 TeV. The results are compared to different types of perturbative QCD calculations.

PACS numbers: 14.70,13.85

1. Introduction

In Leading Order (LO) prompt photons originating in the hard interaction between two partons are produced mainly via quark-gluon Compton scattering ($qg \to q\gamma$) or quark–anti-quark annihilation ($q\bar{q} \to g\gamma$). Studies of direct photons with large transverse momenta, p_T^γ, provide precision tests of perturbative QCD (pQCD) as well as information on the distribution of partons within protons, particularly the gluon. These data are also used in global fits of parton distributions functions (PDFs).

The LO contributions to di-photon production are quark–anti-quark annihilation ($q\bar{q} \to \gamma\gamma$) and gluon-gluon scattering ($gg \to \gamma\gamma$). The latter subprocess involves initial state gluons coupling to the photons through a quark box; thus the subprocess is suppressed by a factor α_s^2. The rate is still high for small $\gamma\gamma$ masses due to the large flux of gluons. Processes where both photons originate from parton fragmentation or where one photon is prompt and one photon is from parton fragmentation also contribute in LO. Di-photon final states are not only interesting to study pQCD but they are also signatures for many new physics processes, such as Higgs production at the LHC or Large Extra Dimensions.

* Presented at the PHOTON2005 conference, September 2005, Warsaw, Poland

DØ has measured the cross section for the inclusive production of isolated photons in the range $23 < p_T^\gamma < 300$ GeV. This extends previous measurements in this energy regime [1–5] to significantly higher values of p_T^γ. CDF has measured the di-photon cross-section in $p\bar{p}$ collisions [6]. Both measurements are restricted to photons in the pseudorapidity range $|\eta| < 0.9$. The data samples correspond to an integrated luminosity of about $L = 326$ pb^{-1} for DØ and $L = 107$ pb^{-1} for CDF.

Photons from energetic π^0 and η mesons are the main background to direct photon production especially at small p_T^γ. Since these mesons are produced inside jets, their contribution is suppressed with respect to direct photons by requiring the photon be isolated from other particles.

2. Prompt Inclusive Photon Production (DØ)

Photon candidates in DØ were formed from clusters of calorimeter cells within a cone. Candidates were selected if there was significant energy in the electromagnetic (EM) calorimeter layers ($> 95\%$), and the probability to have a spatially-matched track was less than 0.1%, and they satisfied an isolation requirement. Potential backgrounds from cosmic rays and leptonic W boson decays were suppressed by requiring the missing transverse energy to be less than $0.7p_T^\gamma$. Four additional variables were input to an artificial neural network (NN) to further suppress background and to estimate the purity of the resulting photon sample. The NN was trained to discriminate between direct photons and QCD as well as electroweak background events. The total number of photon candidates remaining after these requirements is 2.7 million.

The isolated-photon cross section $d^2\sigma/(dp_T d\eta)$ is measured by performing an unsmearing as a function of p_T^γ. This is done by iteratively fitting the convolution of an ansatz function with an energy resolution function. The uncertainty in this correction was estimated using two different ansatz functions and included the uncertainty in the energy resolution. An additional correction was applied to p_T^γ for the difference in the energy deposited in the material upstream of the calorimeter between electrons and photons.

The measured cross section, together with statistical and systematic uncertainties, is presented in Fig. 1a. Sources of systematic uncertainty include luminosity (6.5%), event vertex determination ($3.6\% - 5.0\%$), energy calibration ($9.6\% - 5.5\%$), the fragmentation model ($7.3\% - 1.0\%$), photon conversions (3%), and the photon purity fit uncertainty as well as statistical uncertainties on the determination of geometrical acceptance (1.5%), trigger efficiency ($11\% - 1\%$), selection efficiency ($5.4\% - 3.8\%$) and unsmearing (1.5%). The uncertainty ranges are quoted for increasing p_T^γ. Most of the systematic uncertainties have large ($> 80\%$) bin-to-bin correlations in p_T^γ.

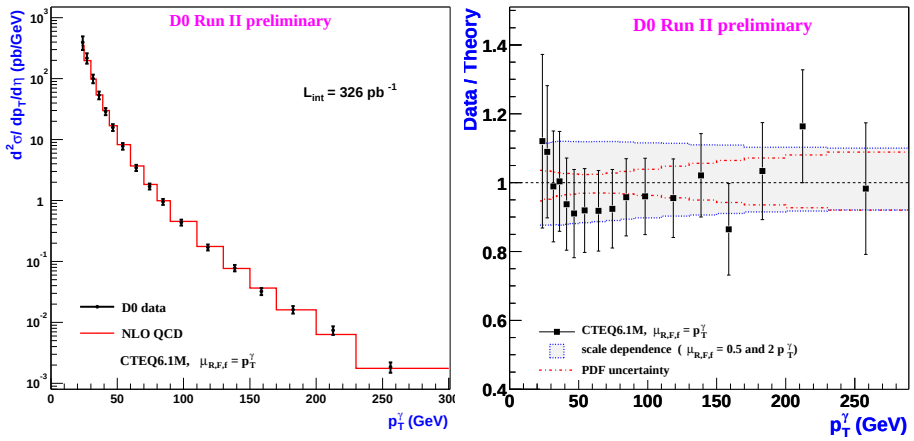

Fig. 1. a) The inclusive cross section for the production of isolated photons as a function of p_T^γ. The results from the NLO pQCD calculation with JETPHOX are shown as solid line. b) The ratio of the measured cross section to the theoretical predictions from JETPHOX. The full vertical lines correspond to the overall uncertainty while the internal line indicates just the statistical uncertainty. Dashed lines represents the change in the cross section when varying the theoretical scales by factors of two. The shaded region indicates the uncertainty in the cross section estimated with CTEQ6.1 PDFs.

Results from a next-to-leading order (NLO) pQCD calculation (JETPHOX [7, 8]) are compared to the measured DØ cross section in Fig. 1a. These results were derived using the CTEQ6.1M [9] PDFs and the BFG [10] fragmentation functions (FFs). The renormalization, factorization, and fragmentation scales were chosen to be $\mu_R = \mu_F = \mu_f = p_T^\gamma$. As shown in Fig. 1b, the calculation agrees, within uncertainties, with the measured cross section. The scale dependence, estimated by varying scales by factors of two, are displayed in Fig. 1b as dashed lines. The span of these results is comparable to the overall uncertainty in the cross section measurement. The filled area represents the uncertainty associated with the CTEQ6.1M PDFs. The central values of the predictions changes by less than 7% when the PDF is replaced by MRST2004 [11] or Alekhin2004 [12]. The calculation is also sensitive to the implementation of the isolation requirements including the hadronic fraction in the $\mathcal{R} = 0.2$ cone around the photon at a level of 3%.

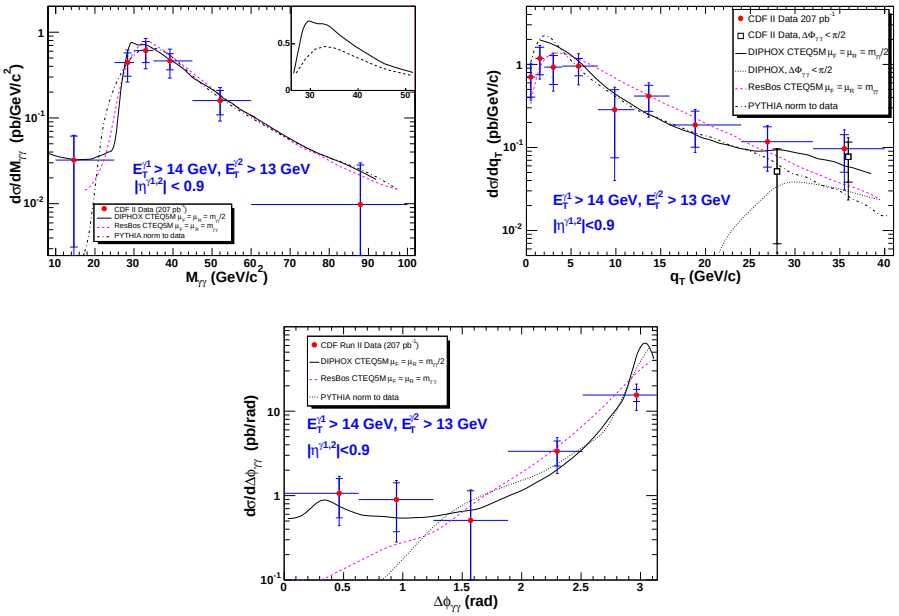

Fig. 2. a) The di-photon differential cross section measured by CDF as function of the invariant mass. The inset shows, on a linear scale, the total NLO cross section from DIPHOX with (solid) and without (dashed) the gluon-gluon contribution. b) The differential cross section as function of the di-photon system p_T (referred as "q_T") Also shown, at larger q_T, are the DIPHOX prediction (dot) and the CDF data (open squares) for the configuration where the two photons are required to have $\Delta\phi < \pi/2$. c) The differential cross section measured by CDF as function of $\Delta\phi$ between the two photons, along with predictions from DIPHOX (solid). The predictions from DIPHOX (solid), RESBOS (dashed), and PYTHIA (dot-dashed) are also shown. The PYTHIA predictions have been scaled up by a factor of two.

3. Prompt Di-Photon Production (CDF)

Photon candidates in CDF were identified by requiring the ratio of the hadronic to EM energy to be less than $0.055 + 0.00045E$, where E is the EM energy. Photon candidates with any associated tracks with $p_T > 0.5$ GeV were rejected and the lateral profile of EM showers in the calorimeter is compared to the profile of electrons measured in a test beam. After the final selection, 889 di-photon events remain, of which 427 ± 59 (stat) are real $\gamma\gamma$ events. This background from neutral mesons such as π^0 and η is determined in each kinematic bin using shower shape variables and hits in the preshower detector.

From these events, the calculated acceptance and the integrated luminosity, CDF has determined the di-photon cross sections for several kinematic variables. The $\gamma\gamma$ mass distribution is shown in Fig. 2a, along with NLO predictions from DIPHOX [7] and RESBOS [13] and from the LO Monte Carlo PYTHIA [14]. DIPHOX is a fixed-order NLO QCD calculation. RESBOS resums the effects of initial state soft gluon radiation. This is particularly important for the distribution of the transverse momentum of the di-photon system, q_T, which is a delta function at LO and divergent as $q_T \to 0$ at NLO. The q_T distribution is shown in Fig. 2b, and the $\Delta\phi$ distribution between the two photons is shown in Fig. 2c. The systematic effects include uncertainties on the selection efficiencies (11%), uncertainties from the background subtraction $(20 - 30\%)$ and from the luminosity determination (6%).

The observed differences between the predictions are expected. The RESBOS q_T prediction is smooth in the entire range, while the DIPHOX curve is unstable at low q_T due to the NLO singularity. The fragmentation contribution in RESBOS is effectively at LO. Since fragmentation to a photon is of order α_{em}/α_s, some 2→3 processes such as $qg \to gq\gamma$, where the quark in the final state fragments to a second photon, are of order $\alpha_{em}^2\alpha_s$ and are included in a full NLO calculation. These contributions are present in DIPHOX, but not in RESBOS, which leads to an underestimation of the production rate in RESBOS at high q_T, low $\Delta\phi$, and low $\gamma\gamma$ mass. In particular, the shoulder at $q_T \approx 30$ GeV arises from an increase in phase space for both the direct and fragmentation subprocesses [15]. The q_T prediction for the $\Delta\phi < \pi/2$ region in Fig. 2b demonstrates that the bump in the DIPHOX prediction at a $q_T \approx 30$ GeV is due to the "turn-on" of the $\Delta\phi < \pi/2$ region of phase space. At $\Delta\phi$ values above $\pi/2$, the effects from soft gluon emission (included in RESBOS but not in DIPHOX) are significant.

The data are in good agreement with the predictions for the mass distribution. At low to moderate q_T and $\Delta\phi$ greater than $\pi/2$, where the effect of soft gluon emissions are important, the data agree better with RESBOS than DIPHOX. By contrast, in the regions where the 2→3 fragmentation contribution becomes important, *i.e.* large q_T, $\Delta\phi$ less than $\pi/2$ and low di-photon mass, the data agree better with DIPHOX.

4. Summary

CDF and DØ have measured prompt photon production using the Run II data taken at the Tevatron with data samples more twice the size of the Run I data. In general, predictions of NLO pQCD are in good agreement with the data in different regions of phase space.

Acknowledgement

Special thanks to Dmitry Bandurin and Michael Begel for their help in preparing these proceedings.

REFERENCES

[1] F. Abe et al., CDF Collab., Phys. Rev. Lett. **73**, 2662 (1994).
[2] B. Abbott et al., DØ Collab., Phys. Rev. Lett. **84**, 2786 (2000).
[3] V.M. Abazov et al., DØ Collab., Phys. Rev. Lett. **87**, 251805 (2001).
[4] D. Acosta et al., CDF Collab., Phys. Rev. D**65**, 112003 (2002).
[5] D. Acosta et al., CDF Collab., Phys. Rev. D**70**, 074008 (2004).
[6] D. Acosta et al., CDF Collab., Phys. Rev. Lett. **95**, 022003 (2005).
[7] T. Binoth et al., Eur. Phys. J. C**16**, 311 (2000).
[8] S. Catani et al., JHEP **05**, 028 (2002).
[9] D. Stump et al., JHEP **10**, 046 (2003).
[10] L. Bourhis et al., Eur. Phys. J. C**2**, 529 (1998).
[11] A.D. Martin et al., Phys. Lett. B**604**, 61 (2004).
[12] S. Alekhin, Phys. Rev. D**68**, 014002 (2003).
[13] C. Balazs et al., Phys. Rev. D**57**, 6934 (1998).
[14] T. Sjöstrand et al., Comp. Phys. Commun. **135** 238 (2001).
[15] T. Binoth et al.,, Phys. Rev. D**63**, 114016 (2003).